# Modeling secondary particle tracks generated by intermediate- and low-energy protons in water

Alexey Verkhovtsev,[1,*] ???,[2] and Gustavo García[1]

[1] *Instituto de Física Fundamental, CSIC, Serrano 113-bis, 28006 Madrid, Spain*

[2] *???*

(Dated: September 30, 2015)

Using an extension of the Low-Energy Particle Track Simulation (LEPTS) Monte Carlo code we model the slowdown of heavy charged particles propagating in water, combined with an explicit molecular-level description of radiation effects due to the formation of secondary electrons, their propagation through the medium, and electron-induced molecular dissociations. As a case study, we consider traverse of protons with the energy from 10 MeV down to 100 eV, i.e. the energy region that contribute mainly to the energy deposition in the Bragg peak region. In order to include protons into the simulation picture, a comprehensive dataset of integral and differential cross sections of elastic and inelastic scattering of intermediate- and low-energy protons from water molecules is created. Experimental and theoretical cross sections available in the literature are carefully examined, compared and verified. The ionization cross section by protons includes recent experimental measurements of the production of different charged fragments.

## I. INTRODUCTION

Understanding radiation effects produced by charged projectiles traversing biological media is of great interest in radiation biology, radiation therapy, and environmental radiation protection. Advantages of ion beam therapy [1–3] over conventional radiotherapy with photons result from a characteristic energy deposition profile as a function of the traversed distance and, as a consequence, from higher relative biological effectiveness of ions as compared to other radiation modalities. The depth-dose profile for ions is characterized by the so-called Bragg peak positioned closer to the end of the ion's trajectory, where a significant amount of energy is deposited into a medium.

An important feature of interaction of ionizing radiation with biological systems is the complexity of biodamage [4]. A thorough understanding of radiation therapy requires evaluation of molecular level effects related to dose deposition on the nanoscale [5, 6]. For that purpose, deep knowledge of numerous interactions induced by charged particles traversing living matter is strongly essential.

It is well understood nowadays that ions traversing a biological medium deposit their kinetic energy by ionizing or exciting molecules of the medium. Secondary electrons and other reactive species which are formed as a result of these processes may interact with biomolecules and produce damage to them [3]. One of the commonly used methods to study these effects in detail is based on Monte Carlo simulations performed by the track structure codes [5, 7–11]. By sampling a sufficiently large number of tracks and averaging over the ensemble obtained, a Monte Carlo simulation can provide, to a high level of accuracy, insights into the mechanisms of the interaction of radiation with matter [4].

A Monte Carlo approach aims at the detailed simulation of trajectories of single particles in a medium, i.e. the complete track structure of the projectile and all secondary particles generated in the medium [12]. Thus, a good quantification of interaction parameters in a wide energy range is required. A common way to precisely determine the physical and chemical events occurring on the nanoscale is to utilize models that can describe energy-loss processes in the medium in terms of interaction cross sections. Being the primary input for track structure codes, such data should include appropriate integral and differential cross sections, energy loss spectra, and scattering cross sections for all kinds of inelastic events, in particular for those leading to molecular dissociations, chemical alterations and radical formation.

By now, it is generally accepted that the great portion of biodamage done by incident ions is related to secondary electrons, free radicals and other reactive species, which are produced by ionizing and exciting the medium [3, 4, 13]. The low-energy electrons, having the kinetic energy from a few eV to several tens of eV, have been shown to act as important agents of biodamage [14, 15]. In particular, it was indicated that electrons with the energy below ionization threshold of a biomolecule can produce damage by dissociative electron attachment [16].

A general limitation of the currently existing Monte Carlo track structure codes is that they often have somewhat inadequate description of the interaction of low-energy electrons with molecular constituents of a medium [17]. Some codes actually stop modeling secondary electrons if their energies drop below 50 eV [18]. In recent years, substantial experimental and theoretical progress has been made to provide the essential data that describe how low-energy electrons interact with the key molecular building blocks of living tissue, such as water and structural components of DNA and RNA [17].

By means of the Low-Energy Particle Track Simulation (LEPTS) code (see the review paper [5] and references therein), it has become possible to model dynamics of

* verkhovtsev@iff.csic.es

secondary species down to the (sub-)electronvolt scale. This Monte Carlo-based tool has been developed to address the molecular level mechanisms of biological damage and to describe radiation effects in nanovolumes in terms of induced molecular dissociations [11]. LEPTS is based on reliable and self-consistent databases of interaction cross sections and energy-loss distributions compiled from experimental data and complemented with theoretical calculations. Up to now, these databases have been available for electrons and positrons and included the following processes for a molecular-level simulation: elastic scattering, ionization, electronic, vibrational and rotational excitations, dissociative electron attachment, neutral dissociation for electrons and positrons, as well as positronium formation and annihilation for positrons [5, 12].

In this paper, we extend the LEPTS methodology to simulate explicitly the slowing-down of heavy charged particles propagating through a biological medium, accounting for the production of secondary particles, including low-energy electrons, and all the induced molecular processes listed above. We focus attention on the simulation of intermediate- and low-energy (from 10 MeV down to 100 eV) protons traversing liquid water that represents the main constituent of living tissue. Charged heavy particles of such energy contribute greatly to the maximum of energy deposition in the Bragg peak region. In order to include protons into the simulations, a comprehensive dataset of integral and differential cross sections of elastic and inelastic scattering of intermediate- and low-energy protons from water molecules is compiled. Experimental and theoretical cross sections available in the literature are carefully examined and verified. The ionization cross section by protons includes recent measurements of the production of different charged fragments and the corresponding classical, semi-classical and *ab initio* calculations. Development of a new database that include adequate data for biologically relevant material provides an opportunity for a realistic, physically meaningful description of radiation damage in living tissue. Hence, the utilized approach allows one to study radiation effects on the nanoscale in terms of the number and the type of induced molecular processes.

## II. ANALYSIS OF THE INPUT DATA

Monte Carlo simulations are based on event-by-event modeling of the interaction between constituent particles of the medium. The input data for the simulations should comprise reliable interaction cross sections and energy loss distributions. In this work, the existing experimental and theoretical data have been critically analyzed and summed up in a set of integral and differential cross sections of elastic and inelastic processes taking place during the slowdown of protons propagating in water.

Generally, a track structure simulation of the charged particle propagation in a biological medium comprises a series of sampling steps that determine the distance between two successive interactions, as well as the type of interaction occurring at the selected point in space. These steps are routinely repeated for all primary and secondary particles until their kinetic energy becomes smaller than a pre-defined cutoff value. The interaction type is randomly selected according to the relative magnitude of the total cross section of all the processes. For the projectile-medium interaction, they are (i) ionization, capture, and excitation induced by a proton, and (ii) ionization, capture, excitation and electron loss induced by a hydrogen atom. The kinematics of the interaction is derived from single- and double-differential cross sections of the corresponding process. Secondary electrons are generated as a result of the ionization event; their energy is defined as the energy lost by the projectile minus the ionization potential of a target molecule. The formation and further evolution of all secondary species is simulated in full according to an explicit database of electron-induced molecular-level interactions that are listed above (see also Ref. [5, 17] and references therein).

One should note that several computer codes for proton transport in water have been reported in the literature so far (e.g., Ref. [7–9]). One of the most recently developed tools is the code called TILDA-V [19], which is based on quantum-mechanically calculated multiple differential and total cross sections for describing inelastic processes occurring during the slowdown of protons in water and DNA. The advantage of the procedure we report here comes from much lower cutoff values for heavy charged projectiles and secondary electrons. In other words, all the particles are explicitly tracked in the simulation until they reach smaller energies; this allows one to get a more consistent picture of the radiation-induced processes occurring on the nanoscale. As noted above, this issue is crucial because low-energy secondary electrons, having the kinetic energy smaller than ionization or even excitation threshold of a water molecule, can produce significant biodamage as a result of dissociative electron attachment. In the TILDA-V code [19], the cutoff energy for protons and neutral hydrogen atoms is fixed to 10 keV, while the cutoff for secondary electrons corresponds to the excitation threshold of a water molecule, that is 7.4 eV. In the simulation performed with LEPTS, the heavy projectiles are tracked down to 100 eV as follows from the data set described in the next section, and the electrons can be tracked until their final thermalization at the sub-eV scale [5, 12].

### A. Integral cross sections

Integral cross sections for elastic and inelastic interactions of 100 eV – 10 MeV protons with water molecules are summarized in Figure 1. Ionization, excitation, and charge transfer (electron capture) were considered as inelastic processes for $H^+$ projectiles (left panel). As a result of the charge transfer process, an electron from a

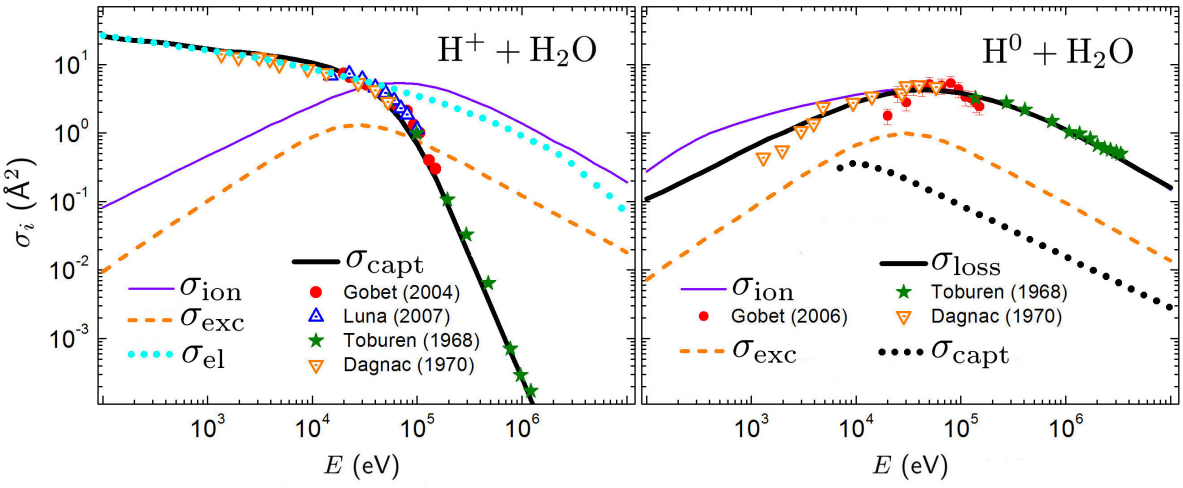


FIG. 1. Integral cross sections for collision of protons with water molecules that have been used as an input for the simulations. Details on data sources are provided in the text. Symbols indicate experimental data from Ref. [20–24]

water molecule is transferred to the moving slow proton to form a neutral hydrogen atom; the corresponding inelastic cross sections for the neutral projectile are shown in the right panel. We have included the processes of ionization and excitation of a water molecule by $H^0$ and also accounted for a probability of electron loss (stripping) and electron capture by the neutral atom; the latter process leads to the formation of a $H^-$ anion.

The ionization cross section by protons has been produced as a result of a careful and thorough analysis of experimental and theoretical data, including recent measurements of the production of different charged fragments [20, 21], and the corresponding classical, semi-classical and *ab initio* calculations [25–27]. The procedure which we have followed to get this set of data is described in detail in Section II B.

The excitation and charge transfer (both electron capture and loss) cross sections for both charged and neutral projectiles were taken from Ref. [19, 28] which are based on a semi-empirical model by Green *et al.* [29, 30]. As indicated in Ref. [28], parameters of the model were chosen to fit the calculated excitation cross sections to those obtained within the first Born approximation at higher projectile energies. We also accounted for elastic scattering of protons from water molecules (nuclear scattering) which becomes important at lower incident energies of about and below 10 keV. Integral elastic cross section data were taken from Refs. [31, 32].

### B. Total ionization cross sections

Data on the total ionization cross section, which have been used in the simulations, are presented in Figure 2. The data set includes the cross section taken from ICRU Report 49, as well as results of experimental measurements. Older experiments done by Rudd and co-workers [33, 34] were focused mainly on determining the total electron production cross section by the integration of their doubly differential electron emission cross sections. More recent experiments [20, 21, 35] allowed one to get the information on production of different charged fragments, namely $H_2O^+$, $H^+$, $OH^+$, and $O^+$. In the compiled data set, we have used these data accompanying with the results of recent theoretical studies [25–27]. In order to get smooth cross sections (shown in Figure 2 by symbols), we did spline interpolation of the experimental data from different measurements [20, 21, 35]. The figure illustrates that the results from the ICRU Report (solid curve) almost coincide with the recent experimental data (filled red circles) at the energies about 10-20 keV and above 1 MeV. In the Bragg peak region, at about 50-100 keV, the new data exceed the already established ones by about 10%. In the compiled data set, we used the new experimental data as a more preferred source. Thus, the resulting curve (shown by a solid purple line in Figure 1) comprises the experimental data [20, 21, 35] in the range 10 keV – 1 MeV and the data from the ICRU 49 Report at lower and higher energies. Note that thus compiled data set is consistent, within the 10% accuracy, with the integrated single-differential cross sections (filled stars in Figure 2), described below.

### C. Differential ionization cross sections

Double-differential cross sections (in terms of the kinetic energy and angular distribution of secondary electrons) for 1.5-, 1.0-, 0.5-, 0.3-, 0.1-MeV, and for 15-keV protons were taken from the experimental data of Toburen and Wilson [36], Bolorizadeh and Rudd [34], and the calculations of Senger and Rechenmann [37]. The cited papers presented the data for secondary electrons with kinetic energy $\varepsilon$ from about 10 eV up to 2.2 keV. These

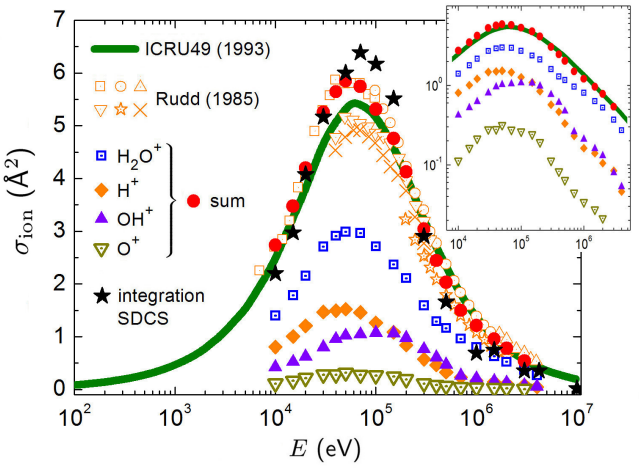


FIG. 2. Total ionization cross sections for collision of protons with water molecules that have been used as an input for the simulations. All symbols except for filled stars indicate experimental data from Ref. [33] and interpolated experimental data from Refs. [20, 21, 35] on the production of charged fragments. Filled stars correspond to the integrated values of single-differential cross sections described in Section II C.

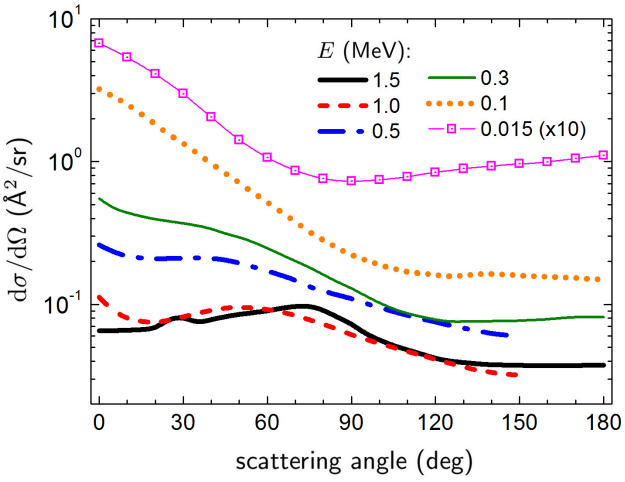


FIG. 3. Single-differential cross section d$\sigma$/d$\Omega$ describing angular distribution of secondary electrons ejected from a water molecule after the collision with protons. See the text for the details on data sources.

data were interpolated, and the compiled dependencies were integrated over the kinetic energy of emitted electrons to get their angular distribution. Thus calculated single-differential (in terms of electron emission angle) cross sections, d$\sigma$/d$\Omega$, are shown in Figure 3.

Single-differential (in terms of kinetic energy of secondary electrons) cross sections, d$\sigma$/d$\varepsilon$, were compiled based on the experimental data from Ref. [34, 38] and supplemented with the calculations from Ref. [9, 28, 39]. A thorough compilation of the data from different sources has allowed us to produce an explicit set of cross sections for 10-, 4.2-, 3.0-, 1.5-, 1.0-, 0.5-, 0.3-, 0.1-MeV and 70-,

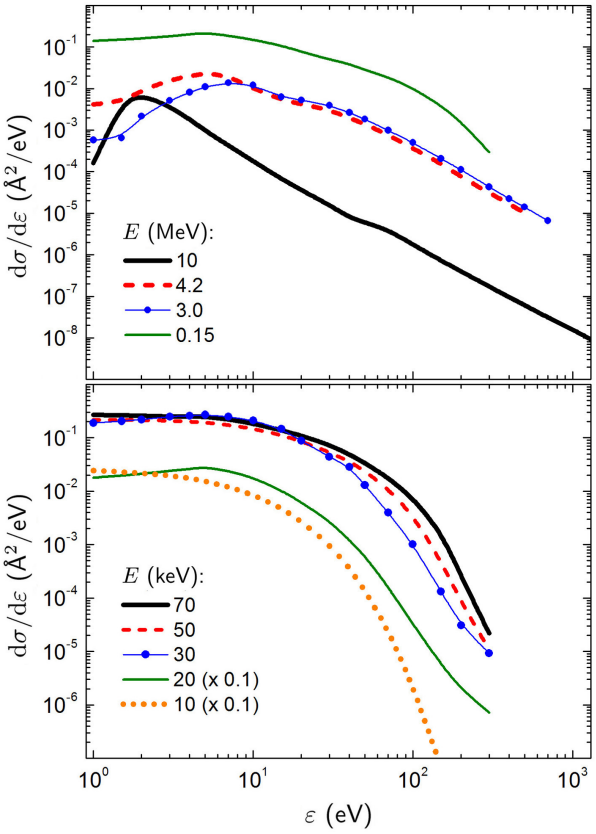


FIG. 4. Energy spectra of secondary electrons, d$\sigma$/d$\varepsilon$, 10 MeV – 10 keV protons, compiled from experimental data [34, 38] and theoretical calculations [9, 28, 39].

50-, 30-, 20-, 15-, and 10-keV protons (see Figures 4 and 5).

### D. Self-consistency of the data set

An important issue of a database created from different experimental and theoretical sources is reliability of the input data. To elaborate on this issue, we have performed several self-consistency checks, namely we compared the integrated double-differential cross sections, $\int \frac{d^2\sigma}{d\Omega d\varepsilon} d\Omega$, with the single-differential cross section, d$\sigma$/d$\varepsilon$, taken from separate sources (see Figure 5) and then also compared the integrated energy spectra $\int \frac{d\sigma}{d\varepsilon} d\varepsilon$ with the total ionization cross section $\sigma_{ion}$ (see Figure 2). The agreement between the differential cross sections is very good, while the relative discrepancy between the integrated d$\sigma$/d$\varepsilon$ and $\sigma_{ion}$ does not exceed 10% confirming the reasonable level of accuracy of the input data for simulations.

## III. RESULTS OF THE SIMULATIONS

TBA

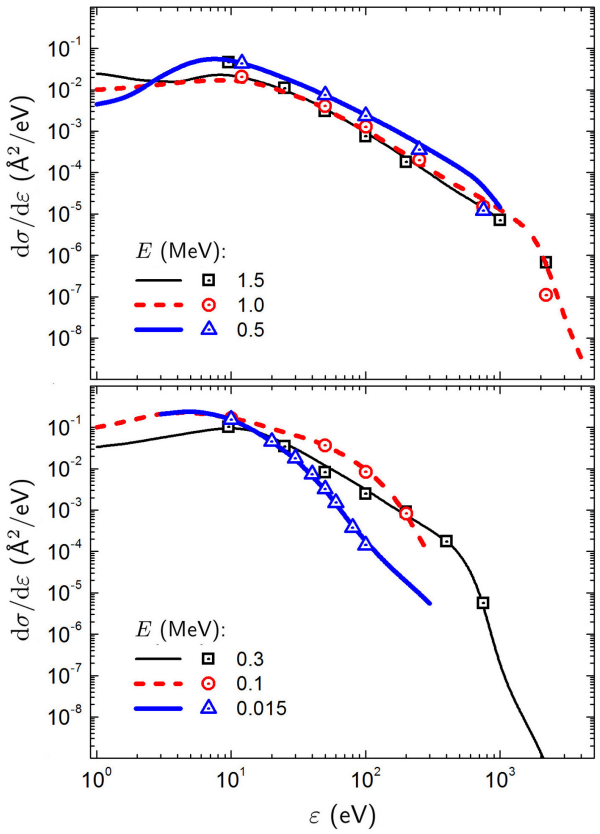


FIG. 5. Same as Fig. 4 but for different projectile energies (solid and dashed curves). Symbols correspond to the integrated values of double-differential cross sections compiled from Ref. [34, 36, 37].

## IV. CONCLUSIONS

TBA

## ACKNOWLEDGEMENTS

The research leading to these results has received funding from the European Union Seventh Framework Programme (PEOPLE-2013-ITN-ARGENT project) under grant agreement no. 608163.

[1] D. Schardt, T. Elsässer, and D. Schulz-Ertner, Heavy-ion tumor therapy: Physical and radiobiological benefits, Rev. Mod. Phys. **82**, 383–425 (2010).
[2] M. Durante and J. S. Loeffler, Charged particles in radiation oncology, Nat. Rev. Clin. Oncol. **7**, 37–43 (2010).
[3] E. Surdutovich and A. V. Solov'yov, Multiscale approach to the physics of radiation damage with ions, Eur. Phys. J. D **68**, 353 (2014).
[4] G. García Gomez-Tejedor and M. C. Fuss, *Radiation Damage in Biomolecular Systems* (Springer Science+Business Media B.V., 2012).
[5] F. Blanco, A. Muñoz, D. Almeida, F. Ferreira da Silva, P. Limão-Vieira, M. C. Fuss, A. G. Sanz, and G. García, Modelling low energy electron and positron tracks in biologically relevant media, Eur. Phys. J. D **67**, 199 (2013).
[6] I. Bacarelli, F. A. Gianturco, E. Scifoni, A. V. Solov'yov, and E. Surdutovich, Molecular level assessments of radiation biodamage, Eur. Phys. J. D **60**, 1–10 (2010).
[7] M. Krämer and G. Kraft, Calculations of heavy-ion track structure, Radiat. Environ. Biophys. **33**, 91–109 (1994).
[8] W. Friedland, P. Jacob, P. Bernhardt, H. G. Paretzke, and M. Dingfelder, Simulation of DNA damage after proton irradiation, Radiat. Res. **159**, 401–410 (2003).
[9] H. Nikjoo, S. Uehara, D. Emfietzoglou, and F. A. Cucinotta, Track-structure codes in radiation research, Radiat. Meas. **41**, 1052–1074 (2006).
[10] S. Incerti, A. Ivanchenko, M. Karamitros, *et al.*, Comparison of Geant4 very low energy cross section models with experimental data in water, Med. Phys. **37**, 4692–4708 (2010).
[11] A. Munoz, J. M. Pérez, G. García, and F. Blanco, An approach to Monte Carlo simulation of low-energy electron and photon interactions in air, Nucl. Instrum. Meth. A **536**, 176-188 (2005).
[12] P. Arce, A. Muñoz, M. Moraleda, J. M. Gomez Ros, F. Blanco, J. M. Perez, and G. García, Integration of the low-energy particle track simulation code in Geant4, Eur. Phys. J. D **69**, 188 (2015).
[13] B. D. Michael and P. O'Neill, A sting in the tail of electron tracks, Science **287**, 1603–1604 (2000).
[14] M. A. Huels, B. Boudaïffa, P. Cloutier, D. Hunting, and L. Sanche, Single, double, and multiple double strand breaks induced in DNA by 3-100 eV electrons, J. Am. Chem. Soc. **125**, 4467–4477 (2003).
[15] B. Boudaïffa, P. Cloutier, D. Hunting, M. A. Huels, and L. Sanche, Resonant formation of DNA strand breaks by low-energy (3 to 20 eV) electrons, Science **287**, 1658–

1660 (2000).
[16] X. Pan, P. Cloutier, D. Hunting, and L. Sanche, Dissociative electron attachment to DNA, Phys. Rev. Lett. **90**, 208102 (2003).
[17] M. C. Fuss, L. Ellis-Gibbings, D. B. Jones, M. J. Brunger, F. Blanco, A. Muñoz, P. Limão-Vieira, and G. García, The role of pyrimidine and water as underlying molecular constituents for describing radiation damage in living tissue: A comparative study, J. Appl. Phys. **117**, 214701 (2015).
[18] A. Muñoz, F. Blanco, J. C. Oller, J. M. Pérez, and G. García, in *Advances in Quantum Chemistry*, edited by J. R. Sabin and E. Brändas (Academic Press, 2007), Vol. 52, pp. 21-57.
[19] M. A. Quinto, J. M. Monti, M. E. Galassi, P. F. Weck, O. A. Fojón, J. Hanssen, R. D. Rivarola, and C. Champion, Proton track structure code in biological matter, J. Phys.: Conf. Ser. **583**, 012049 (2015).
[20] F. Gobet, S. Eden, B. Coupier, J. Tabet, B. Farizon, M. Farizon, M. J. Gaillard, M. Carré, S. Ouaskit, T. D. Märk, and P. Scheier, Ionization of water by (20150)-keV protons: Separation of direct-ionization and electron-capture processes, Phys. Rev. A **70**, 062716 (2004).
[21] H. Luna, A. L. F. de Barros, J. A. Wyer, S. W. J. Scully, J. Lecointre, P. M. Y. Garcia, G. M. Sigaud, A. C. F. Santos, V. Senthil, M. B. Shah, C. J. Latimer, and E. C. Montenegro, Water-molecule dissociation by proton and hydrogen impact, Phys. Rev. A **75**, 042711 (2007).
[22] L. H. Toburen, M. Y. Nakai, and R. A. Langley, Measurement of high-energy charge-transfer cross sections for incident protons and atomic hydrogen in various gases, Phys. Rev. **171**, 114–122 (1968).
[23] R. Dagnac, D. Blanc, and D. Molina, A study on the collision of hydrogen ions $H_1^+$, $H_2^+$ and $H_3^+$ with a water-vapour target, J. Phys. B **3**, 1239–1251 (1970).
[24] F. Gobet, S. Eden, B. Coupier, J. Tabet, B. Farizon, M. Farizon, M. J. Gaillard, S. Ouaskit, M. Carré, and T. D. Märk, Electron-loss and target ionization cross sections for water vapor by 20150 keV neutral atomic hydrogen impact, Chem. Phys. Lett. **421**, 68-71 (2006).
[25] L. F. Errea, C. Illescas, L. Méndez, B. Pons, I. Rabadán, and A. Riera, Classical calculation of ionization and electron-capture total cross sections in $H^+ + H_2O$ collisions, Phys. Rev. A **76**, 040701(R) (2007).
[26] M. Murakami, T. Kirchner, M. Horbatsch, and H. J. Lüdde, Single and multiple electron removal processes in protonwater-molecule collisions, Phys. Rev. A **85**, 052704 (2012).
[27] L. F. Errea, C. Illescas, L. Méndez, and I. Rabadán, Ionization of water molecules by proton impact: Two nonperturbative studies of the electron-emission spectra, Phys. Rev. A **87**, 032709 (2013).
[28] M. Dingfelder, M. Inokuti, and H. G. Paretzke, Inelastic-collision cross sections of liquid water for interactions of energetic protons, Radiat. Phys. Chem. **59**, 255–275 (2000).
[29] A. E. S. Green and R. J. McNeal, Analytic cross sections for inelastic collisions of protons and hydrogen atoms with atomic and molecular gases, J. Geophys. Res. **76**, 133–144 (1971).
[30] J. H. Miller and A. E. S. Green, Proton energy degradation in water vapor, Radiat. Res. **54**, 343–363 (1973).
[31] H. N. Tran, Z. El Bitar, C. Champion, M. Karamitros, M. A. Bernal, Z. Francis, V. Ivantchenko, S. B. Lee, J. I. Shin, and S. Incerti, Modeling proton and alpha elastic scattering in liquid water in Geant4-DNA, Nucl. Instrum. Meth. B **343**, 132-137 (2015).
[32] S. Uehara, L. H. Toburen, and H. Nikjoo, Development of a Monte Carlo track structure code for low-energy protons in water, Int. J. Radiat. Biol. **2** 139-154 (2001).
[33] M. E. Rudd, T. V. Goffe, R. D. DuBois, and L. H. Toburen, Cross sections for ionization of water vapor by 7-4000-keV protons, Phys. Rev. A **31**, 492–494 (1985).
[34] M. A. Bolorizadeh and M. E. Rudd, Angular and energy dependence of cross sections for ejection of electrons from water vapor. II. 15150-keV proton impact, Phys. Rev. A **33**, 888–892 (1986).
[35] U. Werner, K. Beckord, J. Becker, and H. O. Lutz, 3D imaging of the collision-induced Coulomb fragmentation of water molecules, Phys. Rev. Lett. **74**, 1962–1965 (1995).
[36] L. H. Toburen and W. E. Wilson, Energy and angular distributions of electrons ejected from water vapor by 0.31.5 MeV protons, J. Chem. Phys. **66**, 5202–5213 (1977).
[37] B. Senger and R. V. Rechenmann, Angular and energy distributions of $\delta$-rays ejected from low-Z molecular targets by incident protons and $\alpha$ particles, Nucl. Instrum. Meth. B **2**, 204–207 (1984).
[38] W. E. Wilson, J. H. Miller, L. H. Toburen, and S. T. Manson, Differential cross sections for ionization of methane, ammonia, and water vapor by high velocity ions, J. Chem. Phys. **80**, 5631–5638 (1984).
[39] P. de Vera, R. Garcia-Molina, I. Abril, and A. V. Solov'yov, Semiempirical model for the ion impact ionization of complex biological media, Phys. Rev. Lett. **110**, 148104 (2013).